Manuscript Details

Manuscript number	ETFS_2019_1846_R1
Title	Combustion of Crude Glycerol and its Blends with Acetals
Article type	Research Paper

Abstract

In spite of its relevance, the prospective energetic valorization of crude glycerol (CG), a major by-product of biodiesel production, remains nowadays unfulfilled in the industry because of the significant challenges posed by its combustion properties. Besides some basic post-treatments such as desalting (to obtain desalted crude glycerol, DG), its blending with other industrial by-products could improve crude glycerol properties, while maintaining the renewable nature of the fuel. A secondary product obtained from the FAGE process, consisting in a mixture of acetals named GF*, has been proposed in this work as a suitable fuel for this purpose. The combustion characteristics of these by-products have been tested along with different CG-GF* and DG-GF* blends by employing single droplet combustion experiments and semi-industrial furnace tests. Single droplet results point to widely different behaviors between GF* and the glycerols, the latter displaying much lower burning rates and violent microexplosions ascribed to salt content as well as to the broad differences in their constituent's boiling points. Relevant differences were noted between DG and CG modes of microexplosion, presumably due to the lower salt content of the former. Both CG-GF* and DG-GF* mixtures presented similar behaviors to CG, although with a noticeably faster conversion. The furnace tests revealed that GF* addition widened the range of stable conditions in the burner, significantly improving flame stability and reducing CO emissions. NOx emissions slightly increased, although they could be reduced through burner aerodynamics optimization, facilitated by the improvement in flame stability. The reported results support the potential use of GF* as auxiliary fuel for enhancing the combustion behaviors of crude glycerol.

Keywords	Crude Glycerol; Acetals; Semi-industrial Furnace; Droplet Combustion; Microexplosion.
Taxonomy	Combustion, Multiphase Flow, Fluid Mechanics

Corresponding Author	Javier Ballester
Corresponding Author's Institution	LIFTEC - University of Zaragoza
Order of Authors	Álvaro Muelas, Pilar Remacha, Antonio Pina, Jorge Barroso, Álvaro Sobrino, Diego Aranda, Natividad Bayarri, Carles Estévez, Javier Ballester

Suggested reviewers	Jerome Bellettre, William Roberts, Mário Costa

Submission Files Included in this PDF

File Name [File Type]

Cover letter.docx [Cover Letter]

Response_to_reviewers.docx [Response to Reviewers]

Manuscript_highlightedChanges.pdf [Response to Reviewers]

Highlights.docx [Highlights]

Manuscript.doc [Manuscript File]

Declaration-of-competing-interests.docx [Conflict of Interest]

AuthorStatement.docx [Author Statement]

To view all the submission files, including those not included in the PDF, click on the manuscript title on your EVISE Homepage, then click 'Download zip file'.

Title: Combustion of Crude Glycerol and its Blends with Acetals

Authors: A. Muelas[1], P. Remacha[1], A. Pina[1], J. Barroso[1], A. Sobrino[1], D. Aranda[1], N. Bayarri[2], C. Estévez[2] and J. Ballester[1]

Affiliations: [1] LIFTEC, Universidad de Zaragoza/CSIC, María de Luna 10, 50018, Zaragoza, Spain

[2] Inkemia IUCT Group, Álvarez de Castro, 63, 08100 Mollet del Vallés, Spain

Corresponding author:

Javier Ballester

Fluid Mechanics Group

School of Engineering and Architecture

María de Luna, 3, 50018-Zaragoza - Spain

Phone: +34 976 762 153; Fax: +34 976 761 882

ballester@unizar.es

Abstract

In spite of its relevance, the prospective energetic valorization of crude glycerol (CG), a major by-product of biodiesel production, remains nowadays unfulfilled in the industry because of the significant challenges posed by its combustion properties. Besides some basic post-treatments such as desalting (to obtain desalted crude glycerol, DG), its blending with other industrial by-products could improve crude glycerol properties, while maintaining the renewable nature of the fuel. A secondary product obtained from the FAGE process, consisting in a mixture of acetals named GF*, has been proposed in this work as a suitable fuel for this purpose. The combustion characteristics of these by-products have been tested along with different CG-GF* and DG-GF* blends by employing single droplet combustion experiments and semi-industrial furnace tests. Single droplet results point to widely different behaviors between GF* and the glycerols, the latter displaying much lower burning rates and violent microexplosions ascribed to salt content as well as to the broad differences in their constituent's boiling points. Relevant differences were noted between DG and CG modes of microexplosion, presumably due to the lower salt content of the former. Both CG-GF* and DG-GF* mixtures presented similar behaviors to CG, although with a noticeably faster conversion. The furnace tests revealed that GF* addition widened the range of stable conditions in the burner, significantly improving flame stability and reducing CO emissions. NOx emissions slightly increased, although they could be reduced through burner aerodynamics optimization, facilitated by the improvement in flame stability. The reported results support the potential use of GF* as auxiliary fuel for enhancing the combustion behaviors of crude glycerol.

Keywords

Crude Glycerol, Acetals, Semi-industrial Furnace, Droplet Combustion, Microexplosion

Abbreviations

CG - Crude glycerol

DG - Desalted crude glycerol

FAGE - Fatty acid glycerol formal esters
FAME - Fatty acid methyl esters
GF - Glycerol formal
GF* - Mixture of acetals of industrial relevance
NGOM - Non-glycerol organic matter
PG - Pure glycerol

1. Introduction

The extensive manufacture of biodiesel during the last decades has indirectly increased the production of glycerol, a by-product of the transesterification process, where vegetable oils or animal fats react with short-chained alcohols. The obtained glycerol stream, usually denominated crude glycerol, is far from being chemically pure, typically consisting of a mixture of glycerol, water, alcohol, soap, FAMEs and alkaline catalyst residues [1, 2]. These impurities severely hinder its use in high added value processes, being crude glycerol (CG) of very little economic value nowadays [1, 2]. In view of the large surplus of this by-product, and as viable high-end alternatives are very limited with the current refining technologies and market position, its energetic valorization in industrial boilers has been proposed as a feasible solution to the large amounts of CG produced in biodiesel plants.

In principle, the characteristics of CG are compatible with its potential use as fuel in industrial power plants, either completely replacing or co-fired with fossil fuels. Some works in the literature reported favorable results in terms of the co-combustion of glycerol with other fuels (e.g., biomass [1]). Most of those studies analyzed the effect of using glycerol (or other bioliquids) as fuels in small-scale test facilities on the combustion characteristics (specially emitted pollutants) with respect to those obtained from burning traditional fuels (e.g., [3-8]). However, there are still relatively few studies on the use of crude bioliquids in commercial heat/power generation plants [9] due to the modifications required for existing systems [10]. In the case of CG, there are significant differences between its physicochemical properties and those of conventional fossil fuels, namely: low calorific value, high water content, high autoignition temperature, production of toxic acrolein gases, high viscosity at room temperature and high mineral content. These properties significantly hinder the use of CG in combustion-related

applications [3, 4] or may involve significant modifications in existing burners [8, 11]. In particular, the lower calorific value of CG (~16 MJ/kg) compared to that of fossil fuels (e.g. 44 and 46 MJ/kg for diesel and propane, respectively), forces to consume a significant amount of an auxiliary fuel, typically natural gas or propane, to ensure a good quality combustion with stable flame.

An alternative option to overcome the challenges posed by burning neat CG is to blend it with other liquid by-products which can improve its combustion behavior. In doing so, the obtained fuel would be entirely considered as waste-derived, as opposed to its prospective blending with conventional petro-fuels such as diesel. A novel process, described in [12, 13], has been developed to produce Fatty Acid Glycerol formal Esters (FAGE), a fuel of similar characteristics to that of the widespread FAME. This process is reported to yield a by-product consisting in a mixture of acetals, being glycerol formal (GF) the predominant one. This by-product stream is reported to display much more suitable physicochemical properties for its combustion when compared with CG [13], and therefore their potential blending could significantly improve the prospects of a successful valorization of the crude glycerol surplus, while also consuming the aforementioned FAGE by-products. In addition, as detailed in [12, 13], the FAGE manufacture process uses glycerol as feedstock, even further increasing therefore its consumption.

In this work, the combustion characteristics of crude glycerol (as received from a biodiesel plant and also desalted), an acetal mixture (GF*) and their blends were experimentally studied at two different scales. Their combustion properties were obtained under well controlled conditions in single droplet experiments, whereas their behaviors under realistic conditions were assessed from tests in a semi-industrial furnace. The objective was to characterize the behavior of those fuels and to determine the potential benefits of blending crude glycerol, which has been reported to display significant difficulties for its appropriate stand-alone combustion, with GF*.

2. Experimental method

2.1 Fuels investigated

A crude glycerol sample (CG) provided by Mercuria Biofuels as a by-product of their biodiesel manufacture was, after a proper homogenization and filtration process, physicochemically characterized prior to its combustion tests. The main results of this characterization are outlined in Table 1.

Table 1. Main chemical components and properties of the crude glycerol (CG) studied.

Parameter	Value
Glycerol (% m/m)	81.4
Water (% m/m)	2.8
Methanol (% m/m)	0.1
NGOM [a] (% m/m)	7.5
Sulfur (% m/m)	1.1
HHV (MJ/kg)	12.7-15.8 [b]
Density, 30°C (kg/m^3)	1290
Viscosity, 80 °C (cP)	67

[a] Non-Glycerol Organic Matter

[b] The Higher Heating Value was determined four times, with a significant data dispersion (standard deviation of 1.63 MJ/kg). Thus, the upper and lower values, rather than their average, are displayed.

As introduced before, this work aims to explore the possibility of improving the CG combustion characteristics by blending it with a FAGE by-product, consisting in a series of acetal compounds denoted GF and GFOMOM. For the interested reader, information regarding the FAGE, GF and GFOMOM production and characteristics can be found in [12, 13]. A mixture of both by-products was supplied by Inkemia IUCT, in a proportion of industrial relevance for the FAGE production process. This blend was named GF*, and its behavior will be explored along with that of different CG-GF*

mixtures, both in single droplet combustion tests and in the furnace. Three CG-GF* blends were prepared for the droplet experiments, with 7, 15 and 30 vol. % of GF*. In addition, neat glycerol (Panreac, 99.5 % purity) was also included in order to provide a reference baseline.

It is well known that the high mineral content of CG can seriously damage the combustion facilities [5] and for that reason, the 'raw' crude glycerol was processed to remove most of its salt content. Dissolved salts in the CG were removed by solvent precipitation followed by filtration of the solid salts. The solvent was recovered by distillation and reused. With this procedure, the salt content can be reduced up to 80%, depending on the nature of the solvent. The advantage of salt precipitation with respect to the alternative process of glycerin distillation is the lower capital cost of the process equipment. Furthermore, the operating cost of solvent desalting is also lower than glycerin distillation, even if its industrial implementation has several disadvantages (the main one being the need to manipulate the solid salt in the presence of a volatile solvent). Further process optimization is needed in order to successfully scale-up the desalting technology. Even so, this process was applied to a batch of CG, obtaining a representative sample of desalted crude glycerol (DG), whose salt content analysis is compared to that of the original CG in Table 2. Namely, an ICP-AES (Inductively Coupled Plasma Atomic Emission Spectroscopy) analysis was performed at ICB-CSIC in order to quantify the main cations present in both glycerols. This information was complemented with that of the total ash content, measured by means of a burner and a muffle-type furnace. Using this latter parameter as a global indicator of salt presence, the desalination process achieved a reduction of 64.3 % of the total ash content initially present in the CG sample. Once obtained and characterized, the combustion of DG, both neat and blended with GF*, was also analyzed in the droplet facility and in the semi-industrial furnace.

Table 2. Salt content in the crude and desalted glycerol samples.

Parameter	CG	DG
Al (g/kg)	0.013	< D.L. [a]
Ca (g/kg)	0.041	< D.L. [a]
K (g/kg)	25.67	6.00
Na (g/kg)	3.86	3.80
P (g/kg)	1.46	0.38
Ash (% m/m)	7.15	2.55

[a] Detection Limit

2.2 Droplet combustion facility

The single-droplet evaporation and combustion characteristics of the examined fuels were obtained through the Droplet Combustion Facility (DCF) developed at LIFTEC. These experiments provide insight into the intrinsic behavior of each fuel when tested under fixed and well characterized conditions. As these conditions are exactly the same for each sample, the observed differences are completely attributable to the studied fuels, and relative behaviors among them can be extracted in a simplified configuration. A detailed description of the experimental rig used for this purpose can be found elsewhere [14, 15].

The isolated, freely-falling droplets were originated at a piezoelectric device with initial diameters of 151.1±1.9 μm and subsequently injected within a hot coflow, where their evaporation and burning processes were recorded by optical means. In order to decrease the viscosity of the glycerol samples, the droplet generator had to be heated to temperatures up to 100 °C. An interdroplet separation larger than 100 droplet diameters effectively prevented any interaction between droplets [16, 17]. In order to obtain a gaseous ambience representative of those found in real flames, a hot coflow consisting in the combustion products flowing out of a flat-flame burner was used. By adjusting the burner's feed flow rates, the composition and temperature of its exhaust gases could be modified, providing therefore different atmospheres for studying the droplet combustion process. Three conditions were selected, with 0, 3 and 10% of oxygen

molar fraction (dry basis) in the coflow. As in real flames the oxygen availability can significantly vary within flame regions, the chosen conditions are thought to cover a varied range of common ambiences observed by droplets within real spray flames.

The single droplet evaporation and combustion characteristics were entirely gained by means of optical methods. A CCD camera (QImaging Retiga SRV) fitted with a telemicroscope and backlighted through a LED stroboscope used the double exposure technique in order to extract not only the droplets size but also its velocity. With a delay of 500 μs between the LED's shots, a given droplet could be recorded multiple times in the same picture. This is used for measuring the droplet velocity, but also for characterizing other features such as the occurrence of microexplosions. Additionally, a color DSLR camera (Nikon D5000) recorded the visible flame streak formed by the freely-falling droplets, which provided insight into some macroscopically observable features.

2.3 Semi-industrial furnace

The second stage of the combustion tests was conducted in a semi-industrial furnace, under conditions representative of those found in real boilers. The experimental facility has been described in detail in previous works [18, 19] and only their main characteristics will be summarized here.

The combustion chamber is cylindrical and vertically oriented, with a total length of 3.5 m and a diameter of 0.83 m in the upper half, where the burner and the flame are located. All furnace elements are cooled by individual water jackets and their inner walls are refractory lined over the whole chamber length. Fig. 1 shows the geometry of the burner installed in the furnace roof. It was designed to provide a broad flexibility, in order to adapt to different fuels or to implement low-NOx measures (more details in [19]). The combustion air is injected through two concentric ducts, in adjustable proportions; the split was fixed at 68%/32% of primary/secondary air. The liquid fuels were preheated to 80°C and injected by means of an air-assist atomizer. Due to the well-known difficulties to achieve a stable flame with crude glycerol, the facility allowed for the use of an auxiliary fuel (propane), which was injected through 16 injectors installed in the periphery of the burner throat (see Fig. 1). Although the spray characteristics were not determined, mean spray sizes are typically in the order of several tens of microns,

with the distribution tail reaching the order of a hundred microns, as it can be confirmed in [20-21], where the spray characteristics of a heavy oil tested at this same furnace were analyzed. Thus, the droplet sizes used in the single droplets experiments (~150 μm) are expected to be close to the tail of the spray distribution obtained in the current furnace tests.

The main objective of these tests was to evaluate the stability and emissions achievable with crude glycerol (both neat and desalted) and its blends with GF*. Flue gas composition was measured with individual on-line analyzers for O_2, CO and NOx (repeatability < 1%, 0.5 % and 0.5 % of their respective full scale values). Given the lack of generally-accepted methods to evaluate flame stability, some indices were extracted from flame images and radiation. A video camera and a photomultiplier tube fitted with a bandpass filter at 310 ± 5 nm (OH* chemiluminescence band) were installed at one of the side windows with that purpose.

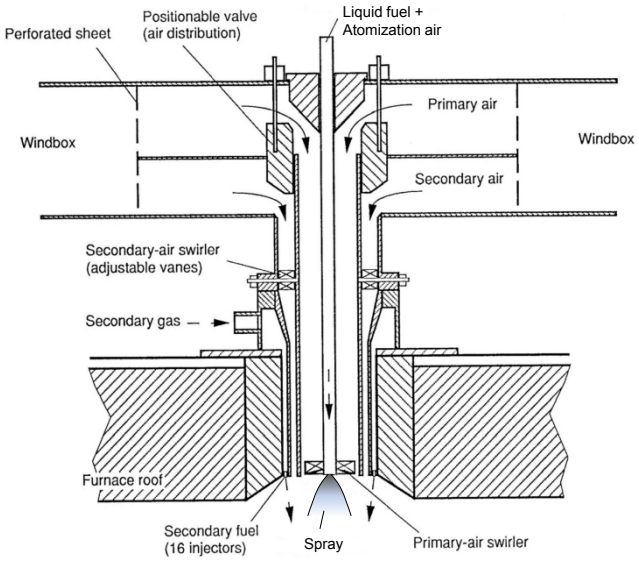

Fig. 1. Burner used for combustion tests in the semi-industrial furnace.

3. Tests in droplet combustion facility

3.1 Base fuels

As introduced in Section 2.1, the droplet evaporation and combustion characteristics of the industrial by-products CG, DG and GF* were extracted along with those of pure glycerol (PG) by means of single droplet tests. These fuels are categorized as 'base

fuels', to distinguish them from the CG-GF* and DG-GF* mixtures, which shall be presented in Section 3.2. Results are displayed in Fig. 2, with the droplet size evolution curves showed in the left column and the subsequently extracted burning rates ($K=-d(D^2)/dt$) provided in the right one. It should be noted that the droplet size curves are normalized by the initial droplet diameter (D_0), so that any small difference in D_0 among tests is automatically corrected. The K-t/D_0^2 curves are obtained as the time-derivatives of the size curves. For this purpose, the latter data was fitted to a 4th order polynomial, which was subsequently derived with respect to time. Regarding the uncertainty of the displayed curves, the error bars for a given droplet residence time have not been included because they are smaller than the symbols used in Fig. 2. Pure glycerol tests were repeated one month after their first run in order to check the procedure repeatability, providing a 6.80, 1.75 and 0.24% difference in time-averaged evaporation rate for the 0, 3 and 10% O_2 conditions, respectively. The first value is unusually high for these tests, which typically show a repeatability in the order of 1% for the time-averaged evaporation rate (e.g., 0.7% for a heating oil vaporization test in [15]). This lower repeatability is thought to respond to the significantly higher initial droplet velocities found for the PG repetition tests (especially for the 0% O_2 case), which would cause a quicker transit of the droplet along the gas coflow temperature profile. Any difference in the gas temperature around the droplet for a given residence time would have a bigger impact in the evaporation experiment, more sensitive towards this parameter because of the absence of a diffusion flame surrounding the droplet. In any case, all the experimental data presented in this work were obtained with initial droplet velocities much closer together than that of PG at the 0% O_2, and therefore their repeatability is expected to be considerably better.

Fig. 2 illustrates very similar evaporative behaviors between CG and PG during approximately the first half of the droplet lifespan for all the studied oxygen conditions. This is ascribed to the high content of glycerol in the studied CG (81.4%, according to Table 1). Both fuels display a prolonged initial heat-up transient with some thermal swelling (i.e., an increase of the droplet size due to its density decrease), primarily caused by their low tendency to evaporate at the droplet's injection temperatures. However, CG appears to show a more volatile behavior in that initial region, with slightly smaller normalized sizes and somewhat higher burning rates. The vaporization of the small fractions of NGOM and water present in the CG (Table 1) is thought to

account for these differences. Over the course of this heat-up period, the PG droplets gradually increase their burning rate until reaching a quasi-steady value which is kept approximately constant until the droplet is completely vaporized, as stated by the well-known d^2-law. The CG curves, by contrast, are suddenly interrupted much before the droplet burnout time due to the onset of violent microexplosions which shattered the droplets. This kind of event was also observed in a previous work on crude glycerol droplet combustion [14], and it is ascribed to the formation of internal vapor bubbles which disrupt the liquid droplet upon their violent release. These disintegrations are reported to be beneficial for the fuel conversion efficiency in real applications, as a secondary atomization would not only significantly shorten the droplets' burnout time, but also improve the fuel-gas mixing within the combustion chamber and reduce pollutant emissions [14, 22]. Just before the microexplosion occurrence, the CG burning rates appear to abruptly decay, departing from the PG behavior. This subtle feature was also noticed in [23] for ethanol-TTIP mixtures, although relevant differences between the microexplosion mechanisms might hamper comparison with the CG case (TTIP was found to hydrolyze creating a solid shell at the surface). A hypothesis which might explain this abrupt decay in K in the present work is based on the results presented by Wang et al. for binary alkane mixtures [17], where it was found that the onset of the first internal vapor bubble occurs much before this event can be inferred from alterations in the droplet size, as the initial bubble size is too small to cause a significant change in the droplet diameter. This initial bubble was reported to grow rather slowly until reaching a turning point, where its size abruptly increased, causing the shattering of the droplet. The progressive decay in the burning rate observed for CG in Fig. 2 could thus be ascribed to the formation of small bubbles inside the droplets just prior to their fragmentation.

On the other hand, the desalted crude glycerol displays a completely different behavior when compared to both CG and PG. As illustrated in Fig. 2, DG droplets underwent an abrupt swelling just after completing their initial heat-up transient. This swelling could rapidly increase the droplet size by a factor of 2 prior to a puffing event or a weak microexplosion. For most cases at the 0 and 3% O_2 conditions, these events achieved to propel some small liquid fragments away from the parent droplet, significantly decreasing its size. After this phenomenon, the DG droplets evaporated smoothly until reaching a new microexplosion, this one analogous to that described for CG, which

completely shattered the droplet. Because of the variable intensity of the weak microexplosions, the DG droplet measurements displayed in Fig. 2 should only be regarded as a sample of the range of sizes observed after this event. Depending on the puffing intensity, the mass loss of the parent droplet varied, explaining therefore the high dispersion found for this particular fuel. This high dispersion hindered the extraction of evaporation and burning rates for DG in Fig. 2. For DG at the 10% O_2 condition, the puffing event was significantly more intense than those described for the 0 and 3% and, for most cases, achieved to shatter the parent droplet into several child droplets of roughly the same size. This fact hampered droplet measurements after the fragmentation point for DG at 10% O_2, as displayed in Fig. 2.

Finally, the acetal mixture GF* presents a much shorter initial heating transient than the glycerols, with substantially higher burning rates throughout the droplet lifespan. Contrary to CG and DG, GF* droplets do not experience microexplosions, and their size evolution curves proceed until the droplets are completely evaporated. In spite of their considerably higher volatility, the total conversion of the GF* droplets is expected to occur slightly after that of crude glycerol, as the shattering of the latter would drastically reduce their consumption time afterwards (combustion time roughly scales with D^2, as it can be noticed in Fig. 2).

When comparing among oxygen conditions for a given fuel, it is clearly ascertained from Fig. 2 that higher oxygen availability accelerates the droplet conversion process, enhancing burning rates and reducing droplet burnout times. This is due to the formation of an envelope flame surrounding the droplet when oxygen is available. If the oxygen fraction in the gaseous coflow is increased, the envelope flame displays a higher temperature and is located closer to the droplet surface. Both effects significantly enhance the heat transfer towards the liquid phase, accelerating therefore the droplet evaporation process and the microexplosion occurrence.

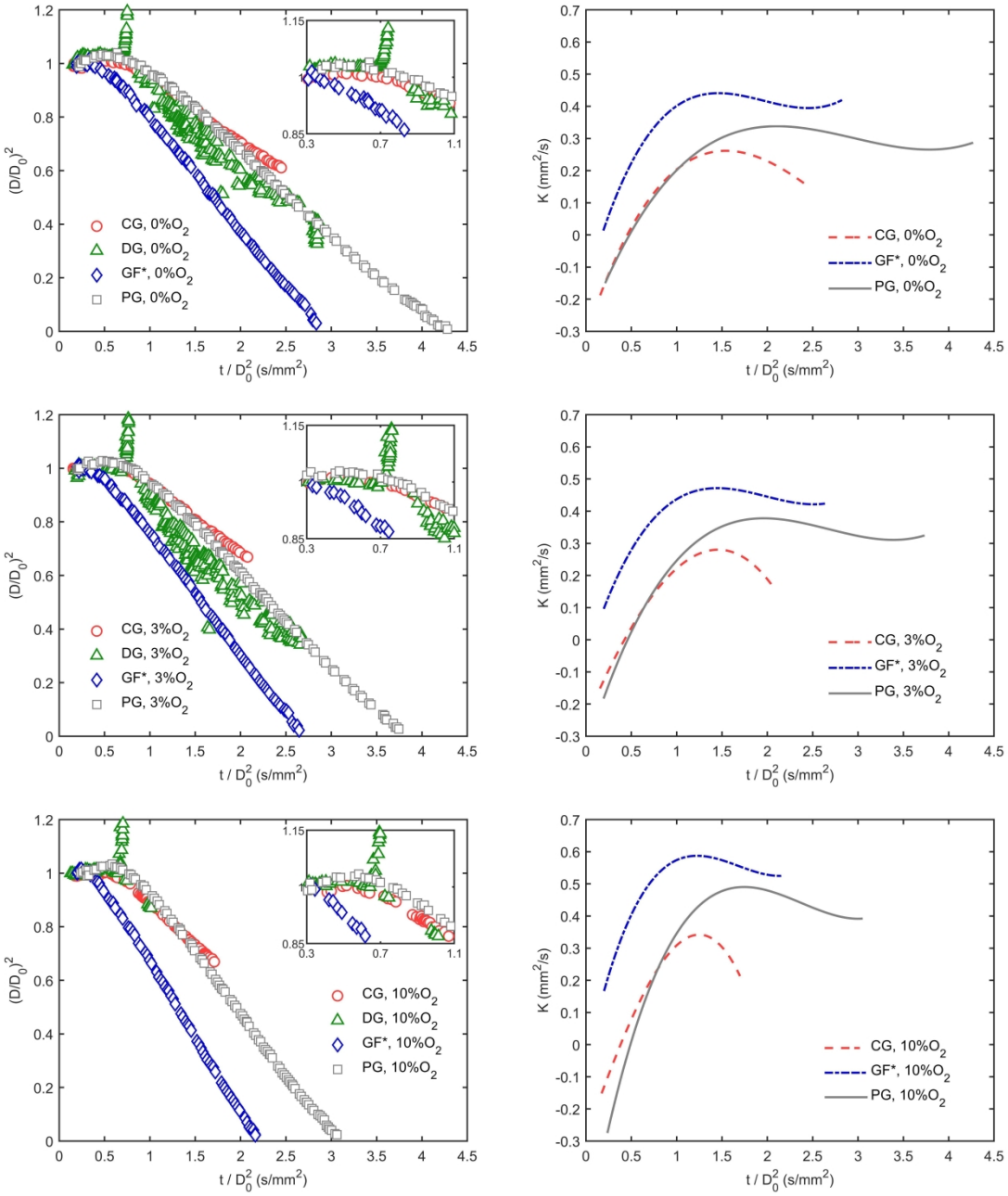

Fig. 2. Normalized droplet size and burning rate evolution for the three studied base fuels at different oxygen conditions (top: 0%, centre: 3%, bottom: 10%).

Fig. 3 illustrates an overview of some microexplosion sequences recorded for CG and DG at the evaporation condition (0% O_2 coflow). As detailed in Section 2.2, each picture displays multiple sequential shots of the same freely-falling droplet 0.5 ms apart. The upper row shows the already described DG swelling and puffing events, whereas the lower one illustrates the CG abrupt microexplosions. The first obvious difference between both is their occurrence point, considerably delayed for CG as it can be

confirmed in Fig. 3. The DG swelling starts just after its heat-up period, with droplet sizes in the order of D_0 (e.g., 153 μm for t/D_0^2=0.708 s/mm^2 in Fig. 3) gradually increasing their diameter during the following few milliseconds (~2 - 4 ms) prior to their break-up and puffing, which can be observed in the triple-exposure pictures at t/D_0^2=0.763 and 0.902 s/mm^2. On the other hand, microexplosions recorded for CG occur after a significant evaporation has already taken place (droplet sizes ~ 120 μm), with a much shorter characteristic time than the swelling and puffing events observed for DG. In the case of CG the upper droplets appear to be totally spherical, without any sign of microexplosion, whereas the lower ones are completely shattered by the bursting of the inner vapors. Therefore, the characteristic time for the recorded fragmentation events would be considerably lower than 0.5 ms for this fuel, even though the initial bubbles might have been building up during a longer time lapse (as observed for a different fuel in [17]). As already pointed out, an additional difference between the two kinds of microexplosions presented in Fig. 3 is the fact that CG microexplosions completely shattered the droplets, whereas the DG break-up phenomena was much weaker, with considerably larger child droplets which could even be tracked and measured downstream the bursting point for the 0 and 3% O_2 conditions (Fig. 2).

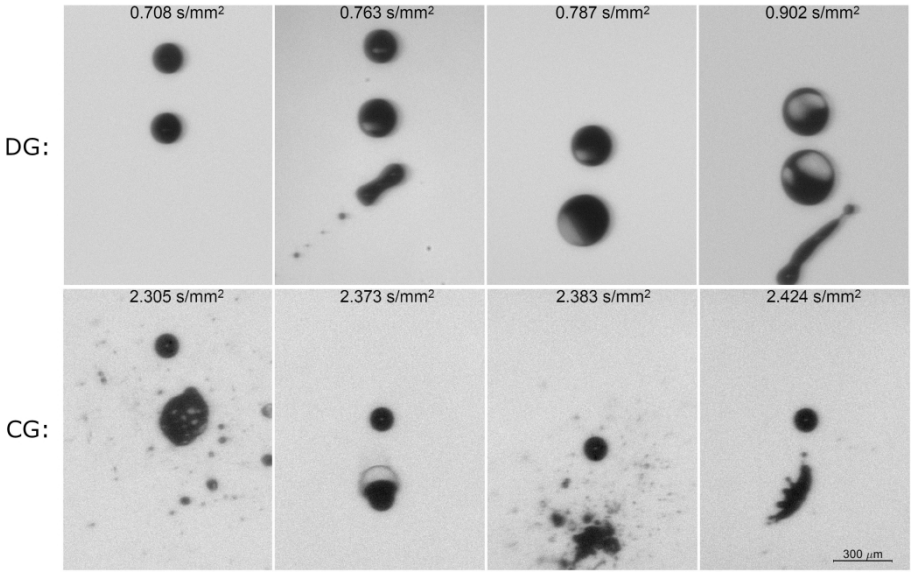

Fig. 3. Droplet swelling and microexplosion sequences for DG (upper row) and CG (lower row) at the 0% O_2 condition. For each sequence, the normalized time after injection (t/D_0^2) for the upper droplet is provided.

The CG microexplosions illustrated in the lower row of Fig. 3 display exactly the same features as those reported in [14] for a different crude glycerol sample, although also with significant differences when compared to [24], another of the few available works on CG droplet combustion. The broad differences between both experimental setups are thought to be responsible for the aforementioned discrepancies, as [24] employed a suspended droplet technique with bigger droplet sizes and lower ambience temperatures. The CG microexplosion typology reported here, with fast (< 0.5 ms) and violent droplet shattering, also differs from those described in several works on different mixtures and emulsions of alkanes, alcohols and water (e.g., [17, 25-27]). All the referred studies, performed by means of the freely-falling technique and avoiding therefore the potential influence of the solid filament, reported the occurrence of significant droplet swelling before its shattering. For instance, binary heptane-hexadecane droplets in [17] were found to increase their diameter by more than 60% prior to droplet burst, with a characteristic time in the order of a few milliseconds. Both microexplosion features appear to closely concur with the DG break-up phenomena illustrated in Fig. 3. Since the experimental configuration used in this work is analogous to that employed in [17, 25-27], the reported DG microexplosions are thought to respond to the same mechanisms proposed in those works, i.e., the homogeneous nucleation of the liquid mixture within the droplet. This local vaporization of the more volatile components (NGOM, water, methanol, even some non-recovered desalination solvent) would create a gas bubble within the liquid phase, whose growth explains the droplet swelling which precedes its break-up. As already discussed, a different case would be that of CG, whose fast and violent microexplosions concur with [14],where the droplet shattering was ascribed to the decomposition of alkali salts rather than to the evaporation of its lighter compounds, following therefore a different mechanism than those governing homogeneous nucleation between liquids. The fact that crude glycerol modifies its original abrupt microexplosions for the slower swelling-induced break-ups after the desalination process also suggests that salt content plays a relevant role in the droplet bursting mode. However, further investigation is clearly needed in order to better ascertain the differences between both microexplosion typologies.

The broad differences noted between the studied base fuels also lead to macroscopically observable distinct behaviors. This can be clearly ascertained from Fig. 4, where the flame traces formed by the combustion of the free-falling droplets are presented by

means of long-exposure photographs. All of them display a subtle blue streak stemming from the chemiluminescent emission of the droplets' envelope flames. However, whereas for pure glycerol and GF* this blue streak spans for the whole droplet burnout time, for CG and DG it is abruptly interrupted by a much more intense orangish emission. This luminosity was analyzed by a spectrometer (Ocean Optics HR2000), which found a marked peak at 589 nm, determining therefore that most of this radiation stems from the emission of excited sodium ions, released after the droplet shattering. This can be verified in Fig. 5, where the spectrum recorded for CG-GF*7 is presented. Thus, the onset of the orangish umbrella in Fig. 4 indicates the point of the first recorded microexplosion for the set of droplets captured in the long-exposure picture. In accordance with the curves presented in Fig. 2, DG droplets experience an earlier occurrence of microexplosions, although this difference is reduced compared to the 0% O_2 condition displayed in Fig. 3. The different modes of droplet shattering can also explain the noticeable differences found between both orangish umbrellas: whereas the CG sodium emission is more centered around a clearly more intense spot, the weaker microexplosions of DG provide a more distributed and asymmetrical sodium release along the child droplets trajectories.

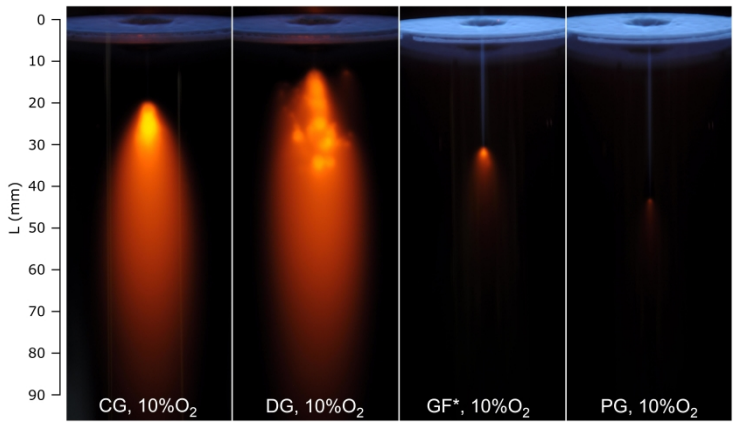

Fig. 4. Macroscopic flame traces created by the freely-falling droplets of the studied base fuels. An exposure time of 2 s was used for GF* and PG, whereas CG and DG pictures were captured with 1/3 s due to their higher luminosity.

The droplet burnout lengths for GF* and PG can also be clearly distinguished in Fig. 4, as they feature an orangish spark at the point of droplet depletion. The spectra recorded determined that these sparks were also caused by sodium emission, and therefore their occurrence is due to small contents of sodium in the GF* and PG, which are released

into the hot ambience after the liquid has completely evaporated. This sodium can either be contained within the original fuel samples or be a result of cross-contamination. In any event, the amount of sodium present in GF* and PG is estimated to be negligible, as the orangish luminosity does not arise until the very instant of droplet depletion. Both the visible flame traces and the recorded spectra point to a negligible soot yield for all the studied fuels, as the characteristic black-body continuum emission ascribed to soot is absent (e.g., see the spectrum recorded for CG-GF*7 in Fig. 5).

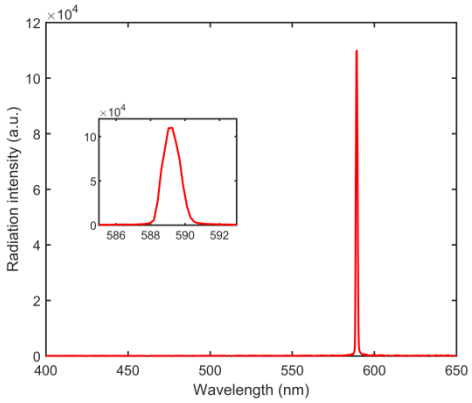

Fig. 5. Emission spectrum recorded in the combustion test of CG-GF*7 droplets (10% O_2 condition).

3.2 Glycerol - acetal mixtures

As introduced before, one of the main objectives of this work is to evaluate the effects of GF* addition on the evaporation and combustion characteristics of crude glycerol. To this end, the tests described in the previous section were performed on different CG-GF* and DG-GF* mixtures at the 3% O_2 coflow condition. The droplet size and burning rate curves are displayed in Fig. 6 for both kinds of blends.

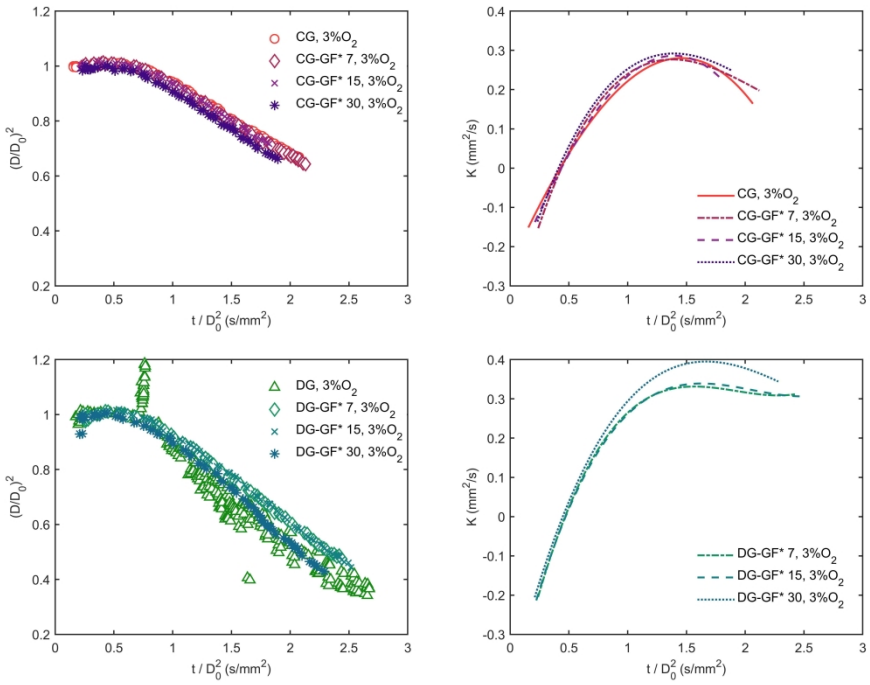

Fig. 6. Normalized droplet size and burning rate evolution for CG-GF* and DG-GF* blends at the 3% O_2 condition.

It is noteworthy that CG and its mixtures with GF* show very similar behaviors throughout all the droplets combustion history. The three studied blends presented the same microexplosion typology than that described for CG in Fig. 3, and their macroscopically observable flame traces were also akin to those recorded for the neat crude glycerol (Fig. 4). Regarding the quantitative evaporation data, it can be inferred from Fig. 6 that GF* addition slightly accelerated the droplet evaporation process, although this effect is barely noticeable for the mixtures with lower GF* content, being clearer for the CG-GF*30 blend.

On the contrary, the addition of GF* drove relevant changes in the combustion features of DG, such as the suppression of the swelling and puffing stages. In [25-27] it was experimentally concluded that, for homogeneous nucleation to occur, the initial concentration of the most volatile constituents (e.g., water, NGOM, non-recovered desalination solvent or methanol in the case of DG) must be within a limited range defined by the relation of the homogeneous superheat limit of the mixture to the boiling point of these less volatile compounds. If, as it was proposed in Section 3.1, the swelling events displayed by DG are indeed caused by homogeneous nucleation within the droplet, the addition of a compound such as GF* could shift the mixture to a

concentration range out of the superheat limits, hindering therefore the initial swelling and puffing phenomena. As it can be noticed in Fig. 6, DG-GF* droplets vaporized smoothly until $(D/D_0)^2 \sim 0.45$, where an abrupt microexplosion led to a complete droplet breakup such as those observed for CG and its mixtures. These kind of microexplosions are ascribed to salt content, and therefore the lower salt concentration of DG is consistent with the delayed occurrence of the droplet shattering for DG-GF* in comparison with CG-GF*, which burst around $(D/D_0)^2 \sim 0.66$. As it was observed for CG mixtures, the burning rate enhancement with GF* blending is more pronounced for a 30% GF* addition, being the evaporation process of DG-GF*7 and DG-GF*15 virtually the same. These results would be in accordance with the behaviors reported for the base fuels in Section 3.1, where the considerably higher volatility of GF*, both in terms of higher burning rates and shorter heat-up periods, was highlighted.

4. Tests in semi-industrial furnace

The combustion characteristics of crude glycerol have been also investigated in a configuration representative of industrial facilities by means of tests performed with CG, DG and their blends with GF* in a semi-industrial furnace. The study has focused on analyzing the range of conditions allowing a stable combustor performance and the need of a support fuel to ensure flame stability. In the tests, the mass flow rate of glycerols, CG-GF* and DG-GF* mixtures was fixed at ~17 kg/h. Propane was used as auxiliary fuel, with flow rates in the range 0-3 Nm^3/h.

A first, basic requirement concerns the stability of the flame, as in many cases glycerol burners need to be supplied with a secondary fuel in order to achieve a stable, attached flame [4, 5, 7]. Thanks to its broad flexibility, the burner used in this study (Fig. 1) could be adjusted to maintain a stable flame without any support fuel. Nevertheless, the operating range and the combustion quality (e.g. in terms of CO emissions) varied with the fuels fed to the burner. For example, in the case of unblended desalted glycerol, DG, a minimum of 5.8% excess oxygen (by vol., dry basis) was needed when no propane was used; this limit gradually decreased with the amount of propane fed through the secondary injectors (see Fig. 1), so that it was below 1.4% for 1 Nm^3/h of propane. The addition of GF* also had a clearly beneficial effect in this respect: the minimum of

5.8% excess oxygen dropped to 2.4% and <3.3%[1] when the proportion of GF* in the liquid fuel was 15% and 30%, respectively. This is a first evidence of the positive effect of blending with GF*, as it could alleviate the need for premium fuels to stabilize the flame.

The CO and NOx emissions measured for the different tests with DG are represented in Fig. 7 and provide a clear picture on the effect of either propane or GF* addition. A limit of 100 ppm was arbitrarily selected as a threshold between 'good' and 'bad' combustion qualities (the legal limit of 1000 ppm is too high for this purpose). Due to the wide range of CO emissions, a logarithmic scale has been used. It should be noted, however, that this magnifies the region of very low emissions (let's say, <20 ppm), where the variations may be due to minor experimental uncertainties and, hence, not always are meaningful.

The use of 0.5 Nm^3/h of propane (Fig. 7, left) leads in all cases to lower CO emissions than if DG or its blends are burned alone. Given the strong influence of excess oxygen on CO and the fact that its range not always overlapped for the different fuels, a direct method to compare the various situations is to determine the oxygen concentration required to keep CO emissions below the 100 ppm threshold. The addition of 0.5 Nm^3/h of propane diminishes in all cases the excess air required to reach the CO limit, the reduction being more marked for DG (<7.3% to 4% O_2) than for DG+15%GF* (4.5% to 3%) and DG+30%GF* (<3.3% to <2.9%). This gradation seems logical, as the margin for improvement is larger for unblended desalted glycerol and gradually narrows as the amount of GF* increases. The positive effect of GF* on combustion quality can be clearly observed by comparing the different curves for fixed propane. The excess oxygen required to keep CO below 100 ppm is a useful index for this purpose: by adding 15% GF*, the oxygen concentration decreases from 4% to 3% for 0.5 Nm^3/h of propane and from >7.3% to 4.5% when no support fuel is used. If the proportion of GF* is increased to 30%, an additional displacement of CO curves to lower excess oxygen is evident for both test series.

[1] Actually, good flame stability was verified with 30% GF*down to 1.5% oxygen, but this was measured in a test with a higher fuel flow rate. Although this does not necessarily affect the result, it was preferred not to include this lower limit in Fig. 7.

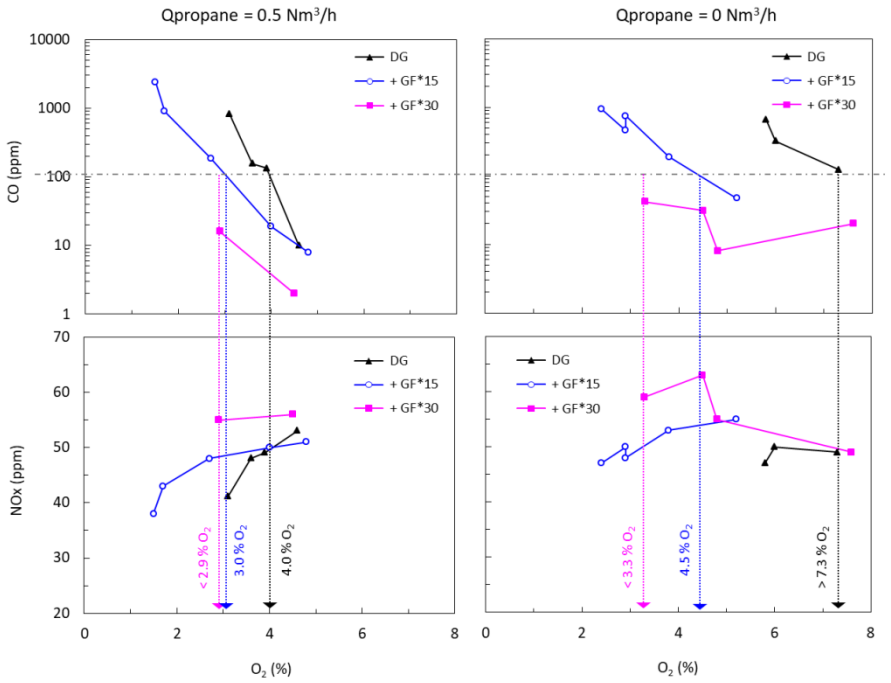

Fig. 7. Emissions of CO (top) and NOx (bottom) measured in the tests with DG and its blends with GF* when burning with 0.5 (left) and 0 Nm³/h (right) of propane. The excess oxygen required in each case for quality combustion (CO<100 ppm) are also indicated.

NOx emissions tend to increase with the amount of GF*. This can perfectly be the consequence of a 'better' combustion (higher temperature, better dispersion of fuel vapor in the air flow). In principle, this could be compensated by modifying the burner aerodynamics (e.g., the split between primary and secondary air), especially when the fuel allows a relatively wide range of stable flame operating conditions, but this was not the objective of the study and no attempt in this regard was made.

As in the case of single droplets tests, the behavior of unblended crude (not desalted) glycerol and the effect of acetals addition were also investigated in the semi-industrial furnace. The results obtained are displayed in Fig. 8 in terms of the CO and NOx emissions measured for the different test series performed with CG, DG ant their corresponding blends with GF*30. The curves show that CG combustion is also improved by GF* addition but this effect is much less intense (for 0.5 Nm³/h of propane, excess oxygen decreases only from <3.4% to 2.5%) than in the tests with DG where a reduction of several orders of magnitude in the CO levels is achieved (Fig. 7).

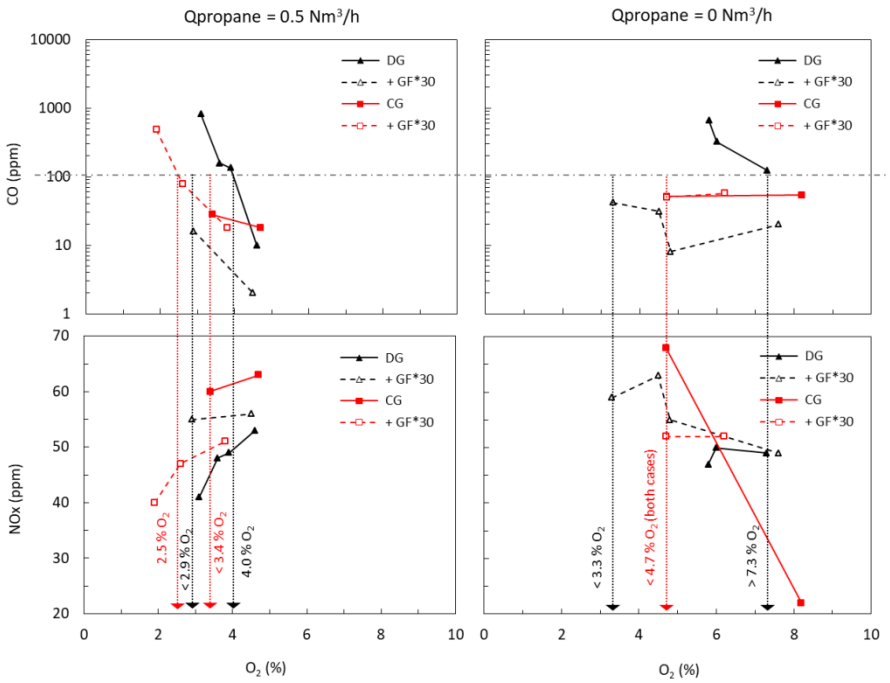

Fig. 8. Emissions of CO (top) and NOx (bottom) measured in the tests with crude and desalted glycerol (CG and DG, respectively) and their blends with 30% GF* when burning with 0.5 (left) and 0 Nm^3/h (right) of propane. The excess oxygen required in each case for quality combustion (CO<100 ppm) are also indicated.

Conversely, it is observed that the desalting process seems to have a negative effect on glycerol combustion as it rises significantly the CO levels, especially when no auxiliary fuel is used: whereas for CG less than 4.7% oxygen is enough to keep CO emissions below the 100 ppm threshold, it must be increased over 7.3% when burning DG. Although the great differences in scale of the facilities used in this work prevents a direct comparison of the results here discussed, this effect could be related to the distinct combustion behavior noticed in the DG droplet tests. As previously explained, DG droplets undergo an initial period characterized by both swelling and puffing events not observed with CG, but the final shattering due to microexplosions is delayed with respect to CG. This is expected to result in a slower and delayed production of fuel vapor in the DG flame, which may also negatively affect the fuel-air mixing and explain the higher excess oxygen required to achieve good flame stability and a nearly-complete conversion to CO_2. In any case, further research would be needed to ascertain these phenomena which are out of the scope of this work.

Information about the flame configuration and appearance was gained from color images recorded with a video camera. The acquisition rate was fixed at 117 fps, resulting in 351 snapshots for each condition, which were subsequently processed to derive a representative mean image. Fig. 9 is an example of the flame appearance for the three fuels tested. The images reflect the commented differences in the combustion behavior, showing brighter flames as the acetal percentage in the mixture is increased. As found for the droplet tests (Fig. 5), the spectrograph confirmed that the orangish color corresponds to the emission band of excited sodium.

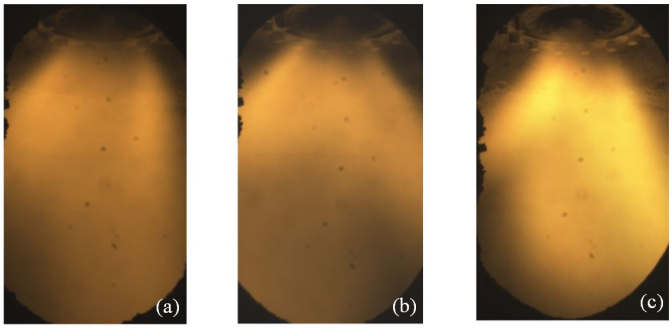

Fig. 9. Flame images with DG (a) and its blends with 15% GF* (b) and 30% GF* (c). 0.5 Nm^3/h of propane in all cases. Oxygen concentrations were 3.6, 4.0 and 2.9%, respectively.

The intensity distribution of each flame image was analyzed and the corresponding axial position of the center of mass was calculated. This parameter, represented in Fig. 10, is indicative of the location of the region where glycerol is burned (since luminosity is dominated by the orange emission due to sodium). In general, the addition of GF* tends to shorten that distance, which seems consistent with an enhanced flame stability. However, it should be noted that when GF* increases from 15% to 30%, the opposite trend is observed; a similar change appears when propane is added. The longer average distance when propane or a high amount of GF* is used might reflect the preferential burning of those more reactive fuels, whereas glycerol combustion (the main origin of the luminosity) is delayed. Therefore, in this case, the location of the visible flame may not always be a reliable stability index. An additional analysis was performed in terms of the amplitude of the oscillations of radiation in the OH* band measured by a photomultiplier. Fig. 10 shows the rms of the photomultiplier signal, normalized by the

mean value. In all cases, the amplitude of the oscillations consistently decreased when either propane or GF* was added, as further confirmation of the improved stability achieved when using a supporting secondary fuel or blending glycerol with acetals.

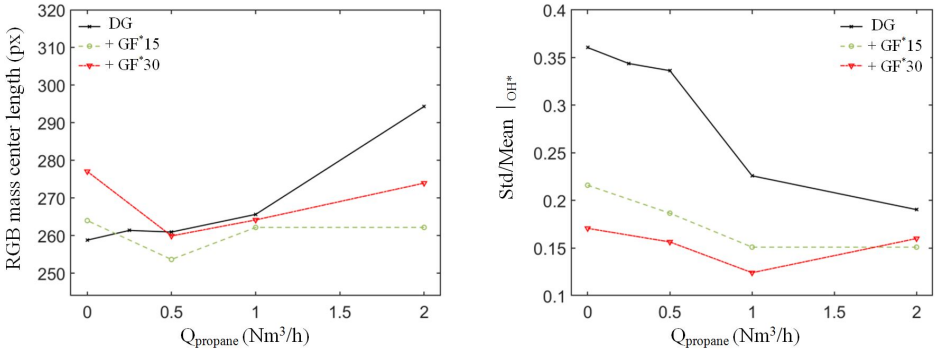

Fig. 10. Axial location of the centre of mass in flame images (left) and the fluctuations level (right) for the flames of DG and its blends with 15% GF* and 30% GF* for different mass flow rates of auxiliary gas (propane). Oxygen concentrations ranged from 2.9% to 6.0%.

5. Conclusions

The combustion characteristics of an industrial crude glycerol sample, both as received from a biodiesel plant (CG) and desalted (DG), were studied along with those of a mixture of acetals named GF* and obtained as a by-product of FAGE production. The effect of GF* addition on the combustion of glycerol was studied at two different scales, namely through single-droplet combustion tests and by means of experiments in a semi-industrial furnace.

The single-droplet combustion tests showed that CG displayed very similar evaporation and burning rates to those of pure glycerol, although the consistent occurrence of microexplosions effectively reduced the CG droplet consumption times. The shattering events were reported to be considerably fast (< 0.5 ms) and violent, with the droplets being practically disintegrated afterwards. Desalted crude glycerol on the other hand, exhibited a completely different behavior, with droplet swelling and puffing just after completing the initial heat-up period, and with a characteristic time in the order of a few milliseconds. These phenomena concur with other single droplet works on liquid mixtures and emulsions under similar experimental conditions, and is therefore ascribed

to the homogeneous nucleation of the most volatile compounds within DG. By contrast, CG microexplosion typology is consistent with that of a previous work, where the salt content was found to be responsible for the shattering events. The acetal mixture GF* displayed a more conventional behavior, with markedly higher burning rates, shorter heat-up initial transients and a smooth and sustained evaporation which lasted until droplet burnout. The addition of GF* did not appear to drive drastic changes in the studied single droplet combustion behaviors for CG, although it suppressed the swelling and puffing stages for DG. In both cases, it progressively increased the burning rates and slightly accelerated the microexplosion onset favoring glycerol conversion.

The combustion behavior of the same fuels (CG, DG and mixtures with GF*) were also tested in a semi-industrial furnace. The results confirmed that the addition of GF* widened the range of stable combustion, significantly reduced CO emissions and notably improved flame stability (as determined from its flickering amplitude), especially in the case of DG. The blends showed a slight increase of NOx emissions, although this might be compensated by optimizing burner aerodynamics (facilitated by the enhanced flame stability). These benefits can also be interpreted from the perspective of a partial or total reduction in the use of premium fuels (natural gas, propane), as GF* can also act as a support fuel, with the advantage of being of renewable nature. In contrast, the results showed that glycerol desalting may result in some increase in the CO levels and, therefore, in the excess oxygen required to reach optimal flame stability and combustion efficiency.

Acknowledgements

This work was financed by the Spanish Ministry of Economy, Industry and Competitiveness and EU FEDER funds through research projects RTC-2016-4618-3 and ENE2016-76436-R, and by the Spanish Ministry of Education through the grant FPU15/01866. The analysis of the glycerol samples was kindly provided by Drs. R. Murillo and M. Callén, from ICB-CSIC. The authors are also grateful to Luis Ojeda for his help in the experimental tasks.

References

[1] J.C. Thompson, B.B. He, Characterization of crude glycerol from biodiesel production from multiple feedstocks, Appl. Eng. Agric. 22 (2006) 261-265.

[2] S. Hu, X. Luo, C. Wan, Y. Li, Characterization of crude glycerol from biodiesel plants, J. Agric. Food. Chem. 60 (2012) 5915-5921.

[3] B. Metzger, Glycerol Combustion, MSc. Thesis, North Carolina State University Raleigh, NC, USA., 2007.

[4] M.D. Bohon, B.A. Metzger, W.P. Linak, C.J. King, W.L. Roberts, Glycerol combustion and emissions, Proc. Combust. Inst. 33 (2011) 2717-2724.

[5] S.A. Steinmetz, J.S. Herrington, C.K. Winterrowd, W.L. Roberts, J.O. Wendt, W.P. Linak, Crude glycerol combustion: Particulate, acrolein, and other volatile organic emissions, Proc. Combust. Inst. 34 (2013) 2749-2757.

[6] P. Queirós, M. Costa, R. Carvalho, Co-combustion of crude glycerin with natural gas and hydrogen, Proc. Combust. Inst. 34 (2013) 2759-2767.

[7] L. Jiang, A.K. Agrawal, Combustion of straight glycerol with/without methane using a fuel-flexible, low-emissions burner, Fuel 136 (2014) 177-184.

[8] W.-C. Huang, S.-S. Hou, T.-H. Lin, Combustion characteristics of a 300 kWth oil-fired furnace using castor oil/diesel blended fuels, Fuel 208 (2017) 71-81.

[9] H. Pawlak-Kruczek, M. Ostrycharczyk, J. Zgóra, Co-combustion of liquid biofuels in PC boilers of 200 MW utility unit, Proc. Combust. Inst. 34 (2013) 2769-2777.

[10] A. Krutof, K. Hawboldt, Blends of pyrolysis oil, petroleum, and other bio-based fuels: A review, Renew. Sustain. Energy Rev. 59 (2016) 406-419.

[11] J.S.J. Alonso, C. Romero-Ávila, L.S.J. Hernández, A.-K. Awf, Characterising biofuels and selecting the most appropriate burner for their combustion, Fuel Process. Technol. 103 (2012) 39-44.

[12] M. Lapuerta, J. Rodríguez-Fernández, C. Estevez, N. Bayarri, Properties of fatty acid glycerol formal ester (FAGE) for use as a component in blends for diesel engines, Biomass Bioenerg. 76 (2015) 130-140.

[13] M. Lapuerta, I. González-García, I. Céspedes, C. Estévez, N. Bayarri, Improvement of cold flow properties of a new biofuel derived from glycerol, Fuel 242 (2019) 794-803.

[14] M. Angeloni, P. Remacha, A. Martínez, J. Ballester, Experimental investigation of the combustion of crude glycerol droplets, Fuel 184 (2016) 889-895.

[15] Á. Muelas, P. Remacha, J. Ballester, Droplet combustion and sooting characteristics of UCO biodiesel, heating oil and their mixtures under realistic conditions, Combust. Flame 203 (2019) 190-203.
[16] T. Li, D. Zhu, N. Akafuah, K. Saito, C. Law, Synthesis, droplet combustion, and sooting characteristics of biodiesel produced from waste vegetable oils, Proc. Combust. Inst. 33 (2011) 2039-2046.
[17] C. Wang, X. Liu, C. Law, Combustion and microexplosion of freely falling multicomponent droplets, Combust. Flame 56 (1984) 175-197.
[18] J. Ballester, J. Barroso, L. Cerecedo, R. Ichaso, Comparative study of semi-industrial-scale flames of pulverized coals and biomass, Combust. Flame 141 (2005) 204-215.
[19] J. Ballester, C. Dopazo, N. Fueyo, M. Hernández, P.J. Vidal, Investigation of low-NOx strategies for natural gas combustion, Fuel 76 (1997) 435-446.
[20] J. Ballester , C. Dopazo , Drop size measurements in heavy oil sprays from pressure-swirl nozzles, At. Sprays 6 (1996) 377–408.
[21] J. Ballester, C. Dopazo, Experimental study of the influence of atomization characteristics on the combustion of heavy oil, Combust. Sci. Technol. 103 (1994) 235-263.
[22] C.R. Shaddix, D.R. Hardesty, Combustion properties of biomass flash pyrolysis oils, Report No. SAND99-8238, Sandia National Laboratories, 1999.
[23] H. Li, C. Rosebrock, N. Riefler, T. Wriedt, L. Mädler, Experimental investigation on microexplosion of single isolated burning droplets containing titanium tetraisopropoxide for nanoparticle production, Proc. Combust. Inst. 36 (2017) 1011-1018.
[24] H.Y. Setyawan, M. Zhu, Z. Zhang, D. Zhang, Ignition and combustion characteristics of single droplets of a crude glycerol in comparison with pure glycerol, petroleum diesel, biodiesel and ethanol, Energy 113 (2016) 153-159.
[25] J. Lasheras, A. Fernandez-Pello, F. Dryer, Experimental observations on the disruptive combustion of free droplets of multicomponent fuels, Combust. Sci. Technol. 22 (1980) 195-209.
[26] J. Lasheras, A. Fernandez-Pello, F. Dryer, Initial observations on the free droplet combustion characteristics of water-in-fuel emulsions, Combust. Sci. Technol. 21 (1979) 1-14.

[27] J. Lasheras, A. Fernandez-Pello, F. Dryer, On the disruptive burning of free droplets of alcohol/n-paraffin solutions and emulsions, Symp. (Int.) Combust. 18 (1980) 293-305.

Manuscript submitted to Experimental Thermal and Fluid Science

Title: **Combustion of Crude Glycerol and its Blends with Acetals**

Authors: **A. Muelas[1], P. Remacha[1], A. Pina[1], J. Barroso[1], A. Sobrino[1], D. Aranda[1], N. Bayarri[2], C. Estévez[2] and J. Ballester[1]**

Affiliations: **[1] LIFTEC, Universidad de Zaragoza/CSIC, María de Luna 10, 50018, Zaragoza, Spain**

[2] Inkemia IUCT Group, Álvarez de Castro, 63, 08100 Mollet del Vallés, Spain

Corresponding author:

Javier Ballester

Fluid Mechanics Group

School of Engineering and Architecture

María de Luna, 3, 50018-Zaragoza - Spain

Phone: +34 976 762 153; Fax: +34 976 761 882

ballester@unizar.es

Declaration of interests

☒ The authors declare that they have no known competing financial interests or personal relationships that could have appeared to influence the work reported in this paper.

☐ The authors declare the following financial interests/personal relationships which may be considered as potential competing interests:

Manuscript submitted to Experimental Thermal and Fluid Science

Title: **Combustion of Crude Glycerol and its Blends with Acetals**

Authors: **A. Muelas[1], P. Remacha[1], A. Pina[1], J. Barroso[1], A. Sobrino[1], D. Aranda[1], N. Bayarri[2], C. Estévez[2] and J. Ballester[1]**

Affiliations: **[1] LIFTEC, Universidad de Zaragoza/CSIC, María de Luna 10, 50018, Zaragoza, Spain**

[2] Inkemia IUCT Group, Álvarez de Castro, 63, 08100 Mollet del Vallés, Spain

Corresponding author:

Javier Ballester

Fluid Mechanics Group

School of Engineering and Architecture

María de Luna, 3, 50018-Zaragoza - Spain

Phone: +34 976 762 153; Fax: +34 976 761 882

ballester@unizar.es

CRediT Author Statement:

A. Muelas: Isolated droplet tests, Analysis of results, Draft preparation
P. Remacha: Isolated droplet tests, Semi-industrial furnace tests, Analysis of results, Draft preparation
A. Pina: Development of experimental facilities, semi-industrial furnace tests
J. Barroso: Semi-industrial furnace tests, Analysis of results
A. Sobrino: Development of experimental facilities, semi-industrial furnace tests
D. Aranda: Isolated droplet tests, Analysis of results
N. Bayarri: Production of fuel samples, Analysis of results
C. Estévez: Conceptualization, Production of fuel samples, Analysis of results
J. Ballester: Conceptualization and supervision, Semi-industrial furnace tests, Analysis of results, Draft preparation